 doi:10.20944/preprints202210.0267.v1

Article

Functionality Analysis of Derailment Containment Provisions through Full-Scale Testing. I: Collision Load & Change in Center of Gravity

Hyun-Ung Bae[1], Kyoung-Ju Kim[1], Sang-Yun Park[2], Jeong-Jin Han[2], Jong-Chan Park[2] and Nam-Hyoung Lim[3*]

[1] R&D Laboratory, Road Kinematics co., Ltd., Cheonan 31094, Korea; bbnine85@gmail.com (H-U.B.);civilkkj@gmail.com (K-J.K.)
[2] Chungnam Railway Research Institute, Chungnam National University, Daejeon 34134, Korea; rwpsy@cnu.ac.kr (S-Y.P.); jjhan0917@cnu.ac.kr (J-J. H.); mioso12@cnu.ac.kr (J-C.P.)
[3] Department of Civil Engineering, Chungnam National University, Daejeon 34134, Korea
*Corresponding; nhrim@cnu.ac.kr; Tel.:+82-42-821-8867

Abstract: In order to reduce the large damage caused by train derailment, protective facilities of various shapes and conditions can be installed on railroad tracks. These protective facilities are referred to as derailment containment provisions (DCPs) and three different types are used worldwide. However, there are no clear standards for DCPs design such as installation location, size, and design load, and performance verification of DCPs installed in the actual railway field is not sufficiently performed. In this paper, the functionality of DCPs is analyzed through the full-scale derailment test. In order to propose a method for estimating the collision load acting on the DCP type I after derailment, the experimental results and simulation results are compared. The function of DCP type I according to the change of the vehicle's center of gravity is identified through comparative analysis of the post derailment behavior.

Keywords: derailment containment provisions; collision load; contact force; center of gravity; train derailment; vehicle body behavior

1. Introduction

A derailment accident of a high-speed train causes a lot of social and economic problems because the damage is very large. Therefore, many countries are taking preventive measures and countermeasures to minimize damage for train derailment accidents. It is difficult to 100% prevent derailment accidents because there are always unpredictable derailment triggers, such as defects in trains and tracks, human error and natural disasters. Therefore, rather than preventing derailment, reducing the large damage caused by derailment can be a more practical and realistic countermeasure. Such technology can be categorized as derailment containment provisions [1,2]. In order to reduce the large damage caused by train derailment, protective facilities of various shapes and conditions can be installed on railroad tracks. These protective facilities are referred to as derailment containment provisions (DCPs) and three different types are used worldwide as shown in Figure 1 [3]. In particular, in DCP Type III, the wheel of the derailed train is primarily controlled by the running rail in the derailing direction and then additionally controlled by the secondary collision with the DCP. In South Korea, DCP Type III is being installed on railway bridges as shown in Figure 2 [4]. It is mandatory for railway lines with a speed of 200 km/hr or higher. However, there are no clear standards for DCPs design such as installation location, size, and design load, and performance verification of DCPs installed in the actual railway field is not sufficiently performed.

Preprints (www.preprints.org) | NOT PEER-REVIEWED | Posted: 19 October 2022 doi:10.20944/preprints202210.0267.v1

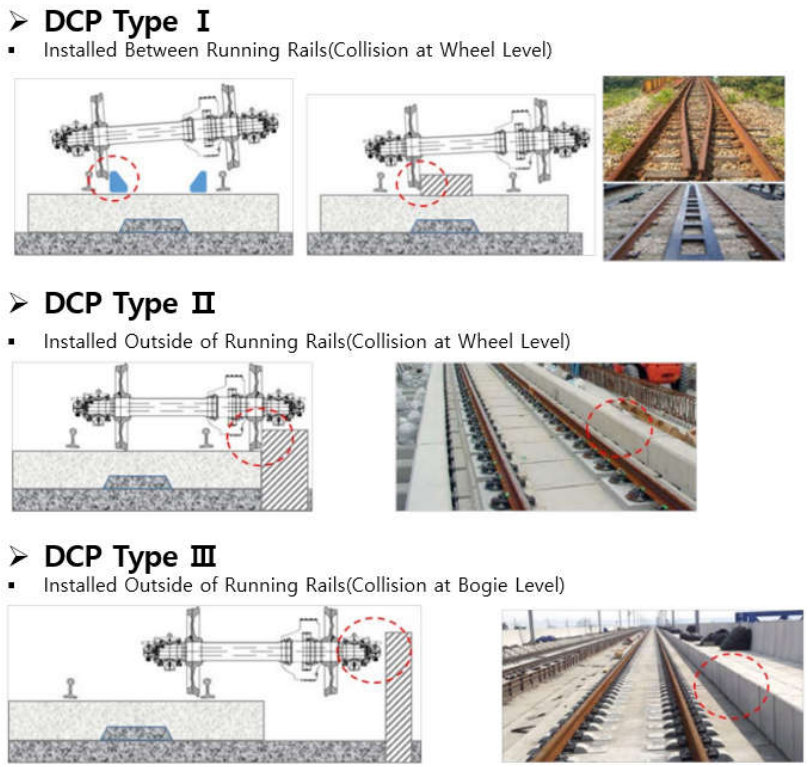

Figure 1. Types of DCPs and their characteristics.

Figure 2. DCPs for high-speed railway bridges in South Korea.

In order to verify the performance of DCPs and to establish generalized design criteria, experimental and analytical studies should be conducted. Barbie et al. [5, 6] analyzed the behavior of the wheels of a derailed train after colliding with concrete sleepers. Wu et al. [7-9] investigated the behavior of railway vehicles after derailment during earthquakes. Bae et al. [1] developed a finite element model for derailment and collision analysis using the LS-Dyna program and evaluated the containment capacity and crashworthiness of the DCP installed in South Korea. Bae et al. [2] analyzed the effect of containment after derailment for various DCP types and suggested the range of possible collision loads for each type. Through such a series of papers, Bae et al. proposed that installation of derailment containment provisions as robust blocks within track gauge (DCP Type I) has many advantages in terms of economics, durability, and efficiency due to the reduction of lateral collision load in comparison with a DCP on the outer side of the track (DCP Type II, III). Song et al. [10] developed a simplified vehicle model that can evaluate the behavior after derailment without significant errors compared to complex vehicle models.

The most reliable way to analyze the behavior of a train after derailment and to evaluate the performance of DCP is to conduct derailment tests on real vehicles. However, since it is very difficult to perform this method, only a few studies have been carried out. Wu et al. [11] analyzed the behavior after derailment based on laboratory-scale derailment test. At the time of derailment, the train speed was 16 km/hr. Bae et al. [12] conducted a derailment test on casting bogie at a real-scale track test site. In this study, the behavior of the bogie after derailment was analyzed in the range of 28-55 km/hr. Song et al. [10], to

Preprints (www.preprints.org) | NOT PEER-REVIEWED | Posted: 19 October 2022 doi:10.20944/preprints202210.0267.v1

verify the developed model, a wagon derailment testing was conducted on a concrete track where DCP type I was installed.

In this paper, the functionality of DCPs is analyzed through the full-scale derailment testing of a freight wagon. The derailment test cars are a flat wagon and container wagon, and a robust concrete block structure in the form of DCP type I is installed on a concrete track. In order to propose a method for estimating the collision(impact) load acting on the DCP after derailment, the experimental results and simulation results using the model developed in previous studies [1, 2, 10] are compared. In addition, the function of DCP type I according to the change of the vehicle's center of gravity is identified through comparative analysis of the post derailment behavior for a flat wagon and container wagon. A comparative study on the characteristics of the derailment behavior for each type of DCPs is performed in the companion paper.

2. Experimental Conditions and Methods

2.1. Real-scale test site

In order to consider the actual conditions of the railway track, a part of the closed railway line was created as a derailment test site [12]. The test site was constructed in three regions as shown in Figure 3.

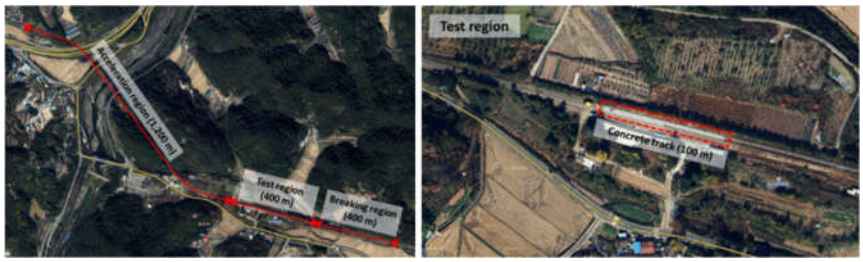

Figure 3. Real-scale test site.

A test concrete track with the same structure and dimension of the Rheda 2000 track on the bridge was installed in the 100 m section of test region as shown in Figure 4a. The robust precast concrete block structure in the form of DCP type I was installed on a 50 m test concrete track. The length, width and height of one unit of this precast concrete block were 2280 mm, 500 mm, and 140 mm respectively as shown in Figure 4b. Each precast concrete block was fixed to the TCL (track concrete layer) using anchors. Also, the additional concrete wall in the form DCP type III shown in Figure 4a was added 2700 mm away from the center of the track to ensure safety after derailment in the case where a DCP type I was not installed within the track gauge.

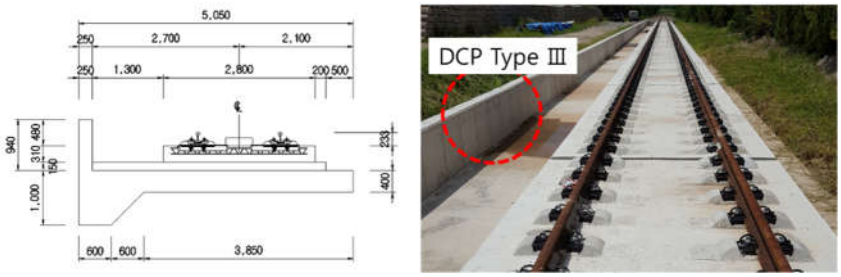

(**a**)

Preprints (www.preprints.org) | NOT PEER-REVIEWED | Posted: 19 October 2022 doi:10.20944/preprints202210.0267.v1

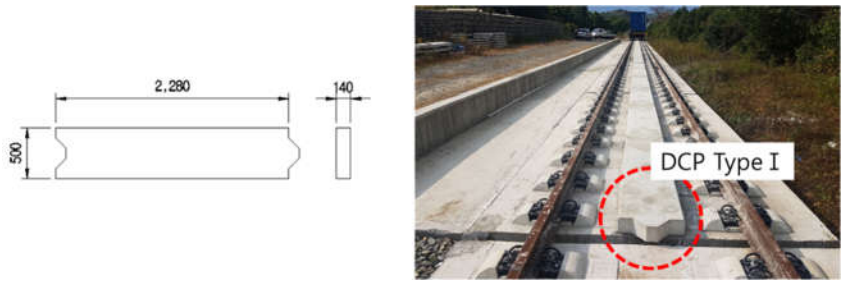

(**b**)

Figure 4. Railway track and DCPs in the test region: (**a**) Rheda 2000 concrete track and (**b**) concrete track with DCP type I.

2.2. Test Car and Acceleration Method

The test freight car units used in this study are a flat wagon and a container wagon as shown in Figure 5. The specification of flat and container wagon is shown in Table 1.

(**a**) (**b**)

Figure 5. Test freight car units: (**a**) flat wagon and (**b**) container wagon.

Table 1. The specification of flat and container wagon.

	Flat wagon	Container wagon
Mass	13030 kg	17320 kg
Weight	127.82 kN	169.91 kN
Length	12590 mm	12590 mm
Width	2330 mm	2330 mm
Height	906 mm	3542 mm
Center of gravity (vertical)	598 mm	1005 mm

A push system was used to accelerate the test car, as shown in Figure 6 [12]. A detailed description of this push system can be found in reference 12.

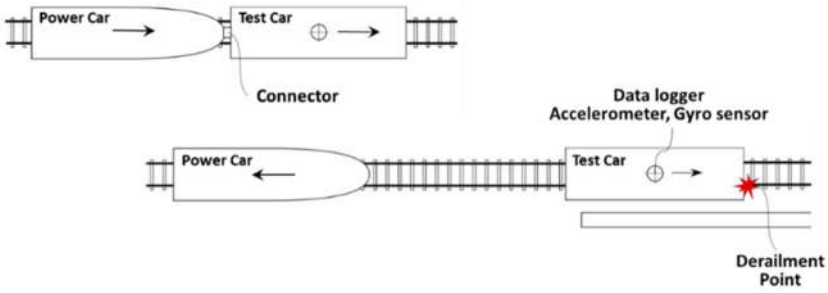

Figure 6. Concept of the push system.

Preprints (www.preprints.org) | NOT PEER-REVIEWED | Posted: 19 October 2022 doi:10.20944/preprints202210.0267.v1

2.3. Derailer System

In this study, the derailment guidance system is designed to forcibly derail the test car by wheel-climbing. The track gauge was forcibly reduced by bending the left rail in the direction of vehicle travel to the inside of the track as shown in Figure 7. Due to the reduced track gauge, the flange of the right wheel of the test car strongly adheres to the head of the right rail in the running direction, and if the friction limit is exceeded, the test car is derailed. In order to make this wheel-climbing easier, the head of the right rail in the running direction was trimmed and oil was applied.

Figure 7. Derailer system.

2.4. Data Acquisition System

The accelerometer, gyro sensors, and shock-resistant datalogger as shown in Figure 8 were installed on the top surface of the wagon body frame. Detailed specifications for the sensor and logger are given in reference 12.

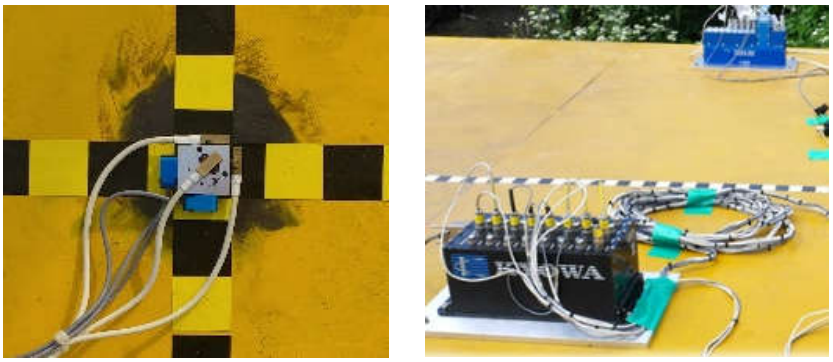

(**a**) (**b**)

Figure 8. Data acquisition system for the test car: (**a**) accelerometers and gyro sensors for the 6-DOF and (**b**) shock-resistant datalogger.

Three high-speed cameras as shown in Figure 9 were used to accurately analyze the train's behavior after derailment. One of the cameras is used with a crane to capture the top view, whereas the other two are used to capture the views from either side. A total of 1000 frames were obtained per 1 s (1000 fps).

Preprints (www.preprints.org) | NOT PEER-REVIEWED | Posted: 19 October 2022 doi:10.20944/preprints202210.0267.v1

Figure 9. High-speed cameras.

3. Experimental Results

The target driving speed immediately before derailment of the test cars was 45–50 km/h. Derailment testing was performed on a flat wagon that DCP type I was installed within track gauge. Also, derailment testing was performed on a container wagon with an increased weight and higher center of gravity under the condition that the same DCP was installed to compare the difference in behavior with the flat wagon.

In order to analyze data such as acceleration measured in an experiment, it is necessary to filter the raw data with unexpected noise. From the previous study [13], it was found that the moving average method derives reasonable results when evaluating collision loads through experiments. In this paper, the measurement data was analyzed by adopting the 50ms moving average method.

3.1. Collision Load

In order to analyze the functionality of DCP, it is necessary to evaluate whether the course of the derailed train is intentionally controlled and whether it robustly resists the impact load caused by the collision with the derailed train. The speed of the flat wagon measured just before the derailment was 51.16 km/h. The derailed wheels collided with the sleeper humps of the concrete track immediately after derailment. Subsequently, the inner wheels continuously collided with the DCP, thereby containing lateral movement, as shown in Figure 10. Through the top-view high-speed camera image, Figure 11 shows more clearly that it prevents the derailed vehicle by DCP installed within track gauge from deviating excessively in the lateral direction.

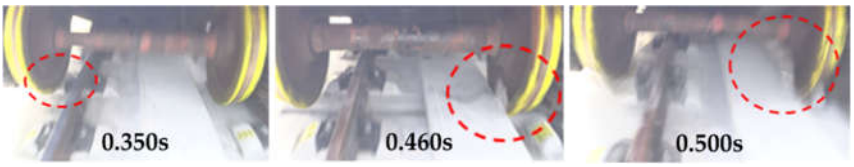

Figure 10. Post-derailment behavior of the flat wagon (1st wheels of front bogie).

Preprints (www.preprints.org) | NOT PEER-REVIEWED | Posted: 19 October 2022 doi:10.20944/preprints202210.0267.v1

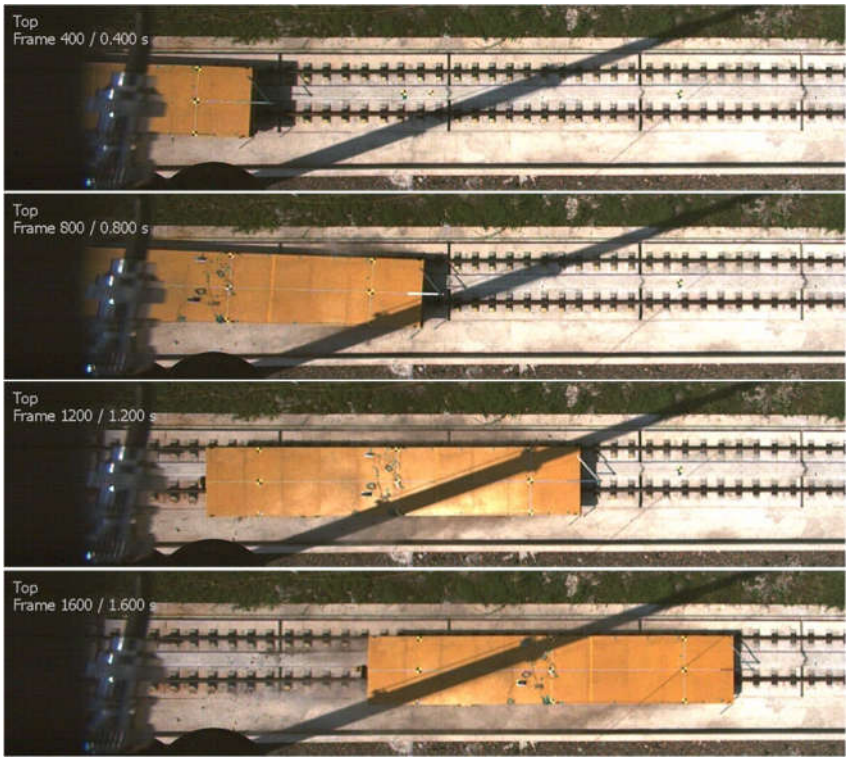

Figure 11. Post-derailment behavior of the flat wagon (top view).

The collision (impact) load through the experiment can be calculated by Newton's second law. In the results of the actual vehicle collision test conducted in previous studies [13], it was analyzed that the magnitude of the collision (impact) load estimated by the vehicle acceleration data may be overestimated. This is because, in the case of a long vehicle such as a trailer, only a portion of the total mass is reflected in the collision load calculation. The collision load through the simulation can be calculated by Newton's second law or from the contact force between the wheel and DCP.

In order to verify the method for calculating the collision load between the derailed train and DCP, the collision load according to Newton's second law and the contact force by the simulation were compared and analyzed. The contact force by the simulation was estimated using the analysis method and simulation model developed and verified in the previous paper [10].

The raw and filtering data using the 50 mms moving average method for the lateral acceleration of the flat wagon through experiments are shown in Figure 12. At 0.49 seconds, the 1st wheel of the front bogie collides with the DCP, and at 0.62 seconds, the 2nd wheel of the front bogie collides with the DCP. The lateral contact force for each wheel obtained through the simulation results is shown in Figure 13. It can be seen that the maximum lateral acceleration and lateral contact force are generated when the 2nd wheel of the front bogie collides with the DCP.

Preprints (www.preprints.org) | NOT PEER-REVIEWED | Posted: 19 October 2022 doi:10.20944/preprints202210.0267.v1

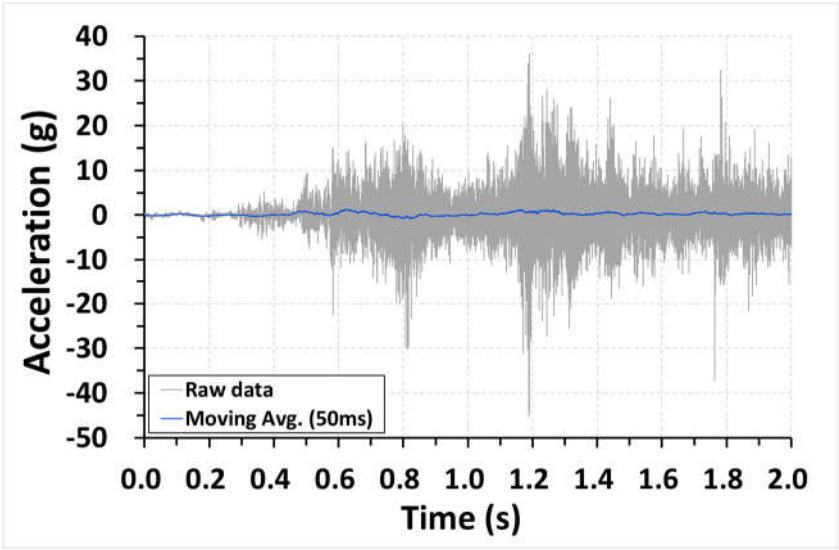

(**a**)

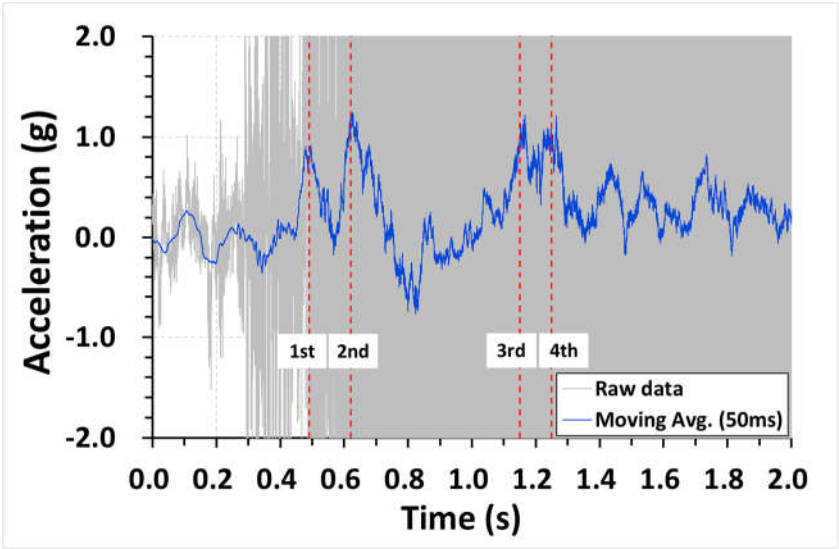

(**b**)

Figure 12. Lateral acceleration of the flat wagon: (**a**) raw and filtering data and (**b**) the point at which the wheels collide with DCP.

Preprints (www.preprints.org) | NOT PEER-REVIEWED | Posted: 19 October 2022 doi:10.20944/preprints202210.0267.v1

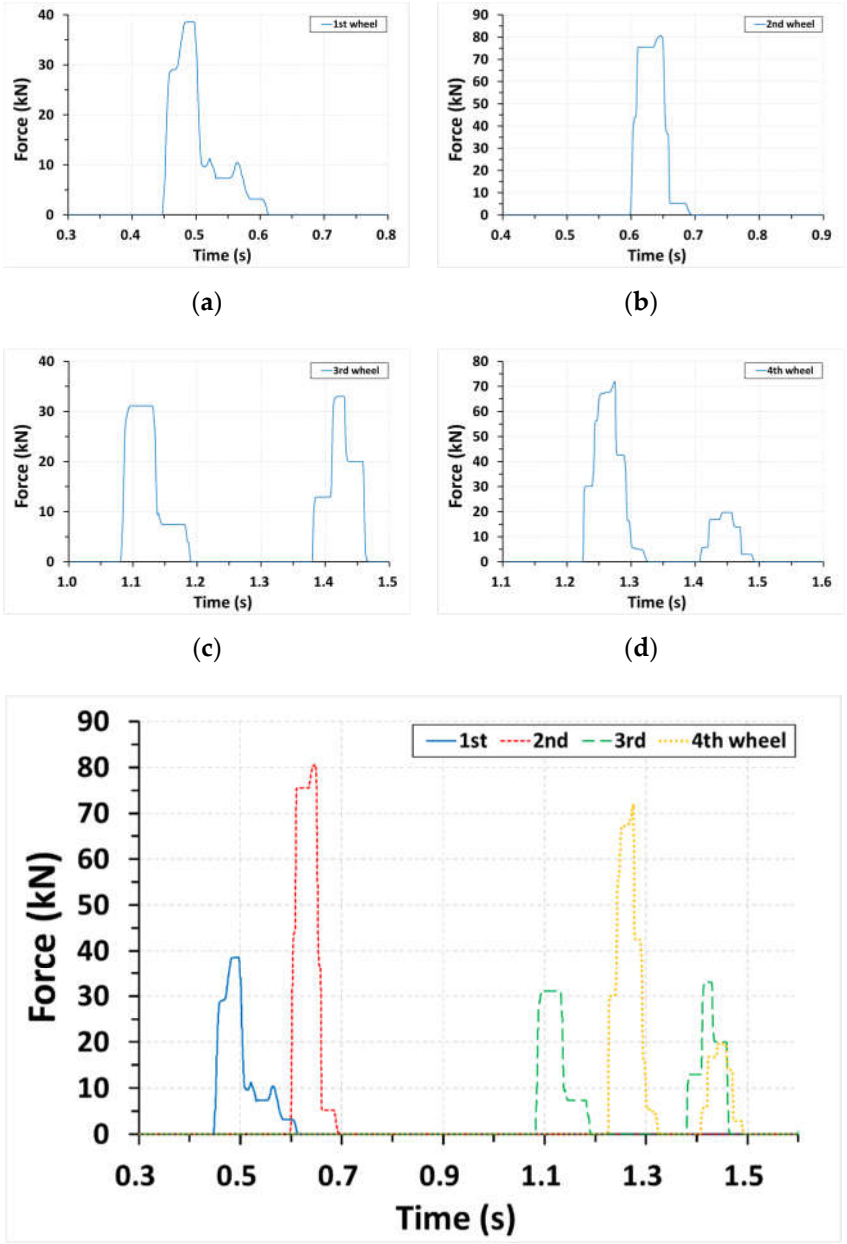

Figure 13. Lateral contact force for each wheel by simulation: (**a**) 1st wheel, (**b**) 2nd wheel, (**c**) 3rd wheel, (**d**) 4th wheel, and (**e**) All wheels.

In the case of the test flat wagon in this study, when the 2nd wheel of the front bogie collides with the DCP after derailing, the rear bogie is still on the rail, so it could be assumed that 50% of the total mass was involved in the collision load. Table 2 shows the comparison of the contact force (simulation result) generated when the 2nd wheel of the front bogie collides with the DCP and the collision load (experimental result) using Newton's second law. In Table 2 and Figure 14, it can be seen that the collision load by the experiment considering only 50% of the total mass agrees well with the contact force by the simulation. That is, when the front bogie of a derailed railway car collides with the DCP, if the rear bogie has not yet derailed, it can be seen that the mass contributing to the maximum collision load at this time is 50% of the mass.

Preprints (www.preprints.org) | NOT PEER-REVIEWED | Posted: 19 October 2022 doi:10.20944/preprints202210.0267.v1

Table 2. Collision load of the 2nd wheel of the front bogie.

Total Mass	Lateral Acceleration	Collision Load using 100% Mass	Collision Load using 50% Mass	Contact Force by Simulation
13030 kg	1.242 g	158.79 kN	79.40 kN	80.57 kN

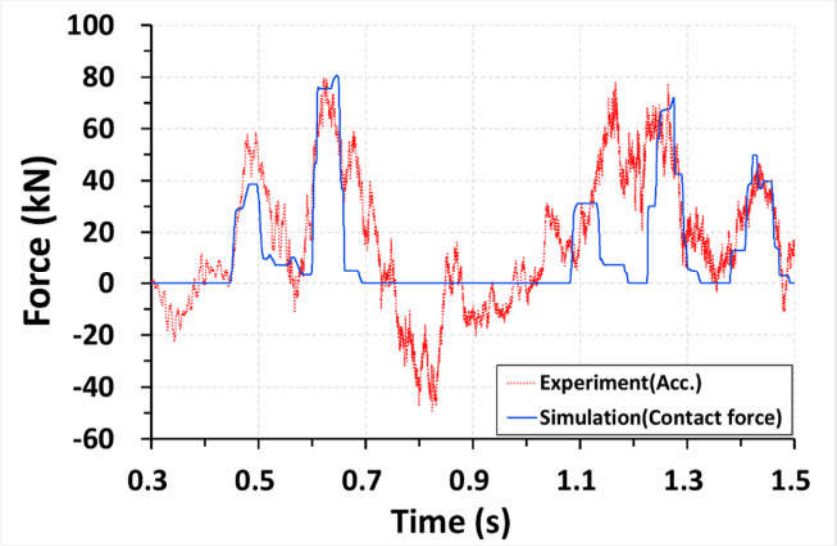

Figure 14. Collision load of the wheels of the flat wagon.

3.2. Change in Center of Gravity

In order to evaluate the effectiveness of the DCP function according to the increase in the vehicle's center of gravity, the additional experiment was conducted with a container wagon. The container wagon weighs 42 kN heavier than the flat wagon and has a center of gravity 407 mm higher than the flat wagon.

The speed of the container wagon measured just before the derailment was 46.69 km/h. As shown in Figure 15, wheels are effectively guided by DCP within track gauge after derailment and are running within the track area. Figure 16 shows the damage condition of DCP at the point of derailment, and although some components at the edges of the DCP side were damaged, we conclude that the DCP effectively performed lateral deviation guiding of the derailed wheels without significant issues. In rare cases, however, if the subsequent train causes continuous repeated collisions at the same damage location, the degree of breakage may be greater, which may lead to degradation in the DCP containment performance. In order to cover the concerns related to these rare events, additional protection facilities such as DCP type II or III are required. In addition, after a derailment accident occurs, it is recommended to evaluate the condition of the damaged DCP panel and replace some damaged DCP panels according to the result.

Preprints (www.preprints.org) | NOT PEER-REVIEWED | Posted: 19 October 2022 doi:10.20944/preprints202210.0267.v1

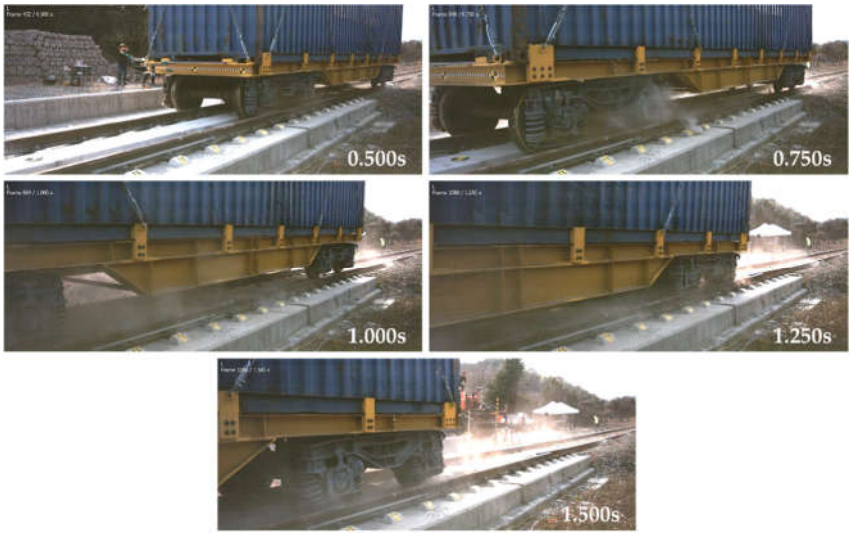

Figure 15. Post-derailment behavior of the container wagon (side view).

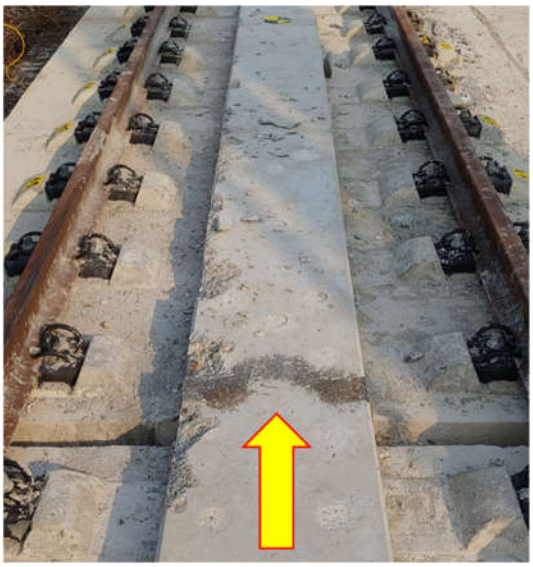

Figure 16. Damage status of DCP after collision.

In order to evaluate the effectiveness of the DCP function according to the increase of the center of gravity, the behavioral characteristics of the flat wagon and the container wagon after derailment were compared. For comparison, the dynamic behavior of the test car considers rolling, pitching and yawing as shown in the Figure 17.

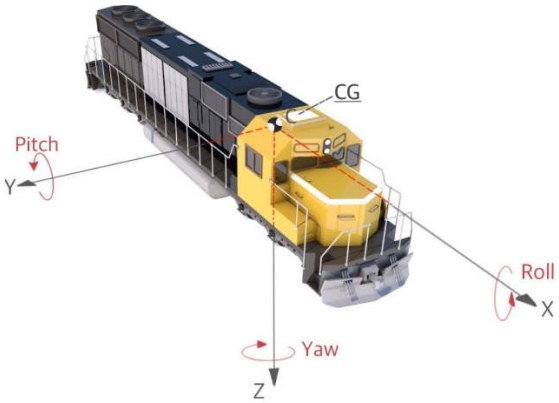

Figure 17. Dynamic behavior of the vehicle.

Preprints (www.preprints.org) | NOT PEER-REVIEWED | Posted: 19 October 2022 doi:10.20944/preprints202210.0267.v1

Figure 18 shows the angle change of the flat and container wagon after derailment. The vehicle angle can be obtained by integrating the angular velocity data measured during the experiment. Figure 18a shows the rolling angle of a flat wagon and a container wagon. Through the analysis of the rolling behavior, it is possible to determine whether the wagon's overturning phenomenon occurs due to a collision with the DCP. The rolling behavior of the container wagon is larger than that of the flat wagon as it swings in the left and right directions of the running direction, but it can be seen that it is gradually stabilized without the overturning phenomenon.

The pitching angle of a flat and container wagon is shown in Figure 18b. The derailed flat wagon is oscillating up and down as it continuously collides with track structures such as sleepers. However, the container wagon, which is heavier than the flat wagon, shows a stabilized pitching behavior even after derailment.

The yawing angle is shown in Figure 18c. The overall length of the container and flat wagon is the same, so when the front bogie collides with the DCP, the yaw angle is equal to about 2.8 degrees. After the derailment of the rear bogie, the yaw angle of the flat and container wagon converges to almost 0 degrees. The slight difference in angle is believed to be due to the speed and weight difference.

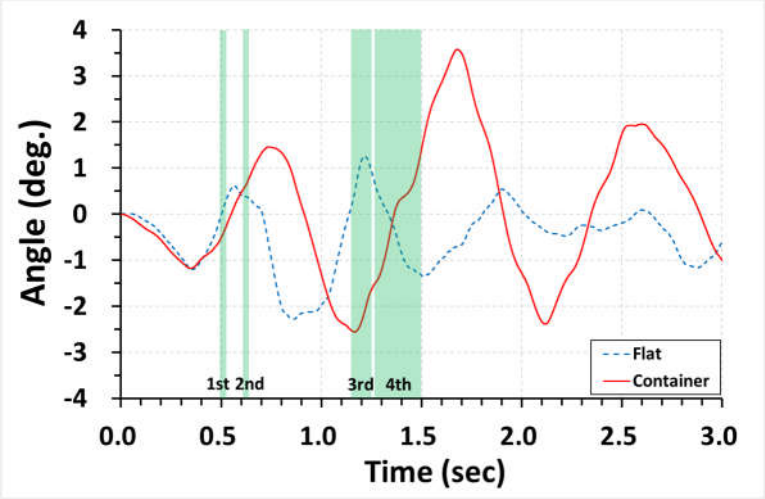

(**a**)

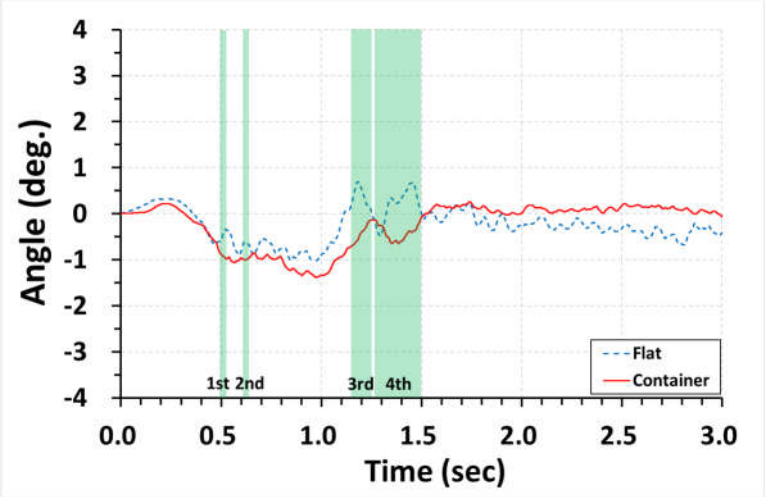

(**b**)

Preprints (www.preprints.org) | NOT PEER-REVIEWED | Posted: 19 October 2022 doi:10.20944/preprints202210.0267.v1

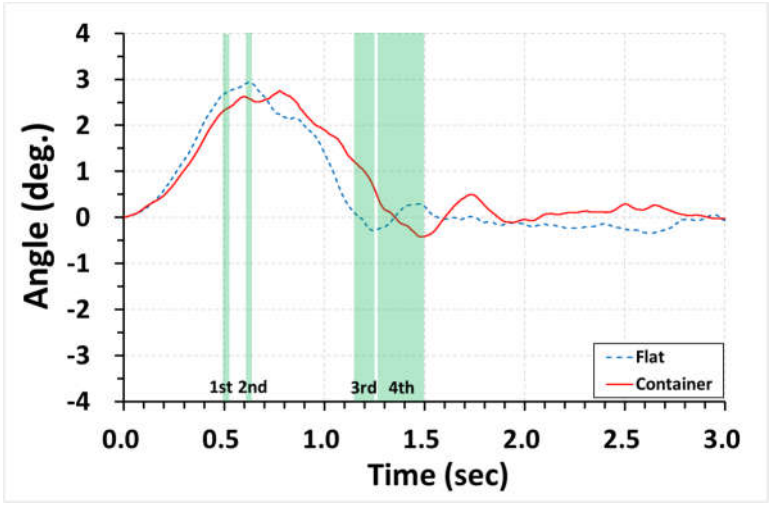

(**c**)

Figure 18. Comparison of vehicle angles after derailment: (**a**) rolling behavior, (**b**) pitching behavior, and (**c**) yawing behavior.

4. Conclusions

In this paper, we analyzed the functionality of DCPs installed within track gauge through the full-scale derailment testing of freight wagon. The main conclusions drawn from this study are as follows:

1. In the case of a long vehicle such as a trailer (railway car), the collision load when the first bogie collides with the DCP can be calculated from Newton's second law applying 50% of the total car mass and lateral car acceleration data.
2. As the sprung mass increases (such as the difference between container wagon and flat wagon), vehicle body behavior (roll, pitch, and yaw) after derailment is different. This is due to the change in mass and center of gravity.
3. Like a container wagon, if the total mass increases and the position of the center of gravity rises, the risk of overturning due to collision with the DCP type I may increase. As a result of comparative analysis of the rolling behavior, it is judged that the DCP's function to restrain the derailed train even if the center of gravity position rises is sufficiently exhibited without any risk of overturning.

Funding: This research was supported by a grant(22TDPP-C163289-02) funded by the Ministry of Land, Infrastructure, and Transport of the Korean government

References

1. Bae, H.U.; Yun, K.M.; Lim, N.H. Containment capacity and crashworthiness estimation of derailment containment wall on high-speed train. *Proc. Inst. Mech. Eng. Part F J. Rail Rapid Transit* **2018**, *232*, 680–696.
2. Bae, H.U.; Yun, K.M.; Moon, J.; Lim, N.H. Impact force evaluation of the derailment containment wall for high-speed train through a collision simulation. *Adv. Civ. Eng.* **2018**.
3. Booz; Allen; Hamilton. Report on the Findings of: Current Practice and Effectiveness of Derailment Containment Provisions on High Speed Lines; HSL-Zuid Organisation: Zoetermeer, The Netherlands, 2004.
4. Korea Rail Network Authority. *Railway Design Guideline and Handbook—Subsidiary and Safety Facilities for Main Lined*; KR C-02060; Korea Rail Network Authority: Daejeon, Korea, 2017.
5. Brabie, D. Wheel-sleeper impact model in rail vehicles analysis. *J. Syst. Des. Dyn.* **2007**, *1*, 468–480.
6. Brabie, D.; Andersson, E. High-speed train derailments—Minimizing consequences through Innovative design. In Proceedings of the 8th World Congress of Railway Research (WCRR 2008), Seoul, Korea, 19–21 May 2008; Union Internationale Des Chemins De Fer (UIC): Paris, France, 2008.
7. Wu, X.; Chi, M.; Gao, H. Post-derailment dynamic behavior of a high-speed train under earthquake excitations. *Eng. Fail. Anal.* **2016**, *64*, 97–110.

 doi:10.20944/preprints202210.0267.v1

8. Wu, X.; Chi, M.; Gao, H.; Ke, X.; Zeng, J.; Wu, P.; Zhu, M. Post-derailment dynamic behavior of railway vehicles travelling on a railway bridge during earthquake. *Proc. Inst. Mech. Eng. Part F J. Rail Rapid Transit* **2016**, *230*, 418–439.
9. Wu, X.; Chi, M.; Gao, H.; Zhang, D.; Zeng, J.; Wu, P.; Zhu, M. The study of post-derailment measures to limit the extent of a derailment. *Proc. Inst. Mech. Eng. Part F J. Rail Rapid Transit* **2016**, *230*, 64–76.
10. Song, I.H.; Kim, J.W.; Koo, J.S.; Lim, N.H. Modeling and Simulation of Collision-Causing Derailment to Design the Derailment Containment Provision Using a Simplified Vehicle Model. *Appl. Sci.* **2020**, *10*, 118.
11. Wu, X.; Chi, M.; Gao, H. The study of post-derailment dynamic behavior of railway vehicle based on running tests. *Eng. Fail. Anal.* **2014**, *44*, 382–399.
12. Bae, H.U.; Moon, J.; Lim, S.J.; Park, J.C.; Lim, N.H. Full-Scale Train Derailment Testing and Analysis of Post-Derailment Behavior of Casting Bogie. *App. Sci.* **2020**, *10*, 59.
13. Beason, W.L.; Hirsch, T.J.; Campise, W.L. Measurement of Heavy Vehicle Impact Forces and Inertia Properties; Final Report, FHWA/RD-89/120; Texas Transportation Institute: College Station, TX, USA, 1989.